

Measurement of NMR Cross-Polarization (CP) Rate Constants in the Slow CP Regime: Relevance to Structure Determinations of Zeolite–Sorbate and Other Complexes by CP Magic-Angle Spinning NMR

Colin A. Fyfe,^{*,‡} Darren H. Brouwer,^{‡,†} and Piotr Tekely[§]

Department of Chemistry, University of British Columbia, 2036 Main Mall, Vancouver BC, Canada V6T 1Z1, and Laboratoire de Méthodologie UMR CNRS 7565, Université Henri Poincaré, Nancy 1, 54500 Vandoeuvre-les-Nancy, France

Received: April 13, 2005; In Final Form: May 24, 2005

When analyzing $I \rightarrow S$ variable contact time cross-polarization (CP) curves, the spin dynamics are usually assumed to be describable in the “fast CP regime” in which the growth of the S spin magnetization is governed by the rate of cross polarization while its decay is governed by the rate of I spin $T_{1\rho}$ relaxation. However, in the investigation of the structures of zeolite–sorbate and other complexes by polarization transfer this will not necessarily be the case. We discuss the measurement of $I \rightarrow S$ CP rate constants under the “slow CP regime” in which the rate of $T_{1\rho}$ relaxation is fast compared to the rate of cross polarization, leading to a reversal of the usual assumptions such that the rate of growth is governed by the rate of I spin $T_{1\rho}$ relaxation while the decay is governed by the rate of cross polarization (and the S spin $T_{1\rho}$ relaxation). It is very important to recognize when a system is in the slow CP regime, as an analysis assuming the normal fast CP will lead to erroneous data. However, even when the slow CP regime is recognized, it is difficult to obtain *absolute* values for the CP rate constants from fits to standard CP curves, since the CP rate constant is correlated to the scaling factor, the contribution from ^{29}Si $T_{1\rho}$ relaxation is ignored, and it is difficult to obtain reliable data at very long contact times. The use of a $^{29}\text{Si}\{^1\text{H}\}$ CP “drain” or “depolarization” experiment, which measures absolute values of the CP rate constants, is therefore proposed as being most appropriate for these situations. To illustrate the importance of these observations, measurements of the ^1H – ^{29}Si CP rate constants in the *p*-dichlorobenzene/ZSM-5 sorbate–zeolite complex by $^{29}\text{Si}\{^1\text{H}\}$ CP and CP drain magic-angle spinning (MAS) NMR experiments are presented and compared and used to determine the location of the guest sorbate molecules in the cavities of the host zeolite framework.

Introduction

We have recently developed an approach to determine the locations of organic sorbate molecules in highly siliceous zeolite frameworks from solid state $^{29}\text{Si}\{^1\text{H}\}$ cross-polarization (CP) magic-angle spinning (MAS) NMR data.^{1–5} With the peaks in the ^{29}Si MAS NMR spectra assigned to crystallographically inequivalent Si sites in the zeolite framework by a two-dimensional ^{29}Si INADEQUATE correlation experiment,^{6,7} it is possible to determine the locations of the sorbate molecules from the relative rates of cross polarization between the ^1H nuclei of the organic sorbate molecules and the ^{29}Si nuclei of the zeolite framework.

However, care must be taken in determining the CP rate constants. The dynamics of cross polarization are usually assumed to be describable in the “fast CP regime” in which the growth of the S spin magnetization is governed by the rate of cross polarization while its decay is governed by the rate of I spin $T_{1\rho}$ relaxation since most polarization transfer experiments involve nearest neighbor (often covalently bonded) bonded nuclei under moderate $T_{1\rho}$ relaxation. However, due to the presence of paramagnetic molecular oxygen in the channels and

cavities of the zeolite,⁸ the ^1H and ^{29}Si spin lock relaxation times ($T_{1\rho}$) can be quite short while the CP time constants (T_{CP}) are quite long since the dipolar interactions between the ^1H nuclei of the sorbate molecules and the ^{29}Si nuclei of the zeolite framework are quite weak and can be further averaged by molecular motions of the guests. When it occurs, this combination of short $T_{1\rho}$ relaxation times and long CP time constants is termed the “slow CP regime”⁹ and leads to complications in the analysis of the CP dynamics that must be recognized to extract the correct CP rate constants to be used for the structure determination.

In a recent paper, Klur et al. emphasized the importance of recognizing the slow CP regime when analyzing CP dynamics to properly measure the relative populations of chemically or crystallographically inequivalent sites from the peak intensities obtained by CP MAS NMR.⁹ It was shown for $^1\text{H} \rightarrow ^{29}\text{Si}$ CP MAS experiments on silica gel and calcium silicate hydrates that, in addition to obtaining erroneous dynamic parameters, incorrect measurements of the populations of the various Si sites result if the $^1\text{H} \rightarrow ^{29}\text{Si}$ CP curves are analyzed assuming the “usual” fast CP regime. The authors proposed the TORQUE experiment¹⁰ as a useful tool to distinguish between the fast and slow CP regimes and to identify multicomponent behavior of the CP dynamics.^{9,11}

The focus of this paper is on the measurement of CP rate constants in the slow CP regime. In addition to further demonstrating the importance of recognizing the slow CP

* To whom correspondence should be addressed. E-mail: fyfe@chem.ubc.ca.

‡ University of British Columbia.

† Present address: School of Chemistry, University of Southampton, Southampton SO17 1BJ, United Kingdom.

§ Université Henri Poincaré.

regime, it is shown that it is very difficult to obtain *absolute* CP rate constants from a CP curve under these circumstances. The CP drain experiment is proposed for measuring absolute CP rate constants. This approach is demonstrated for the determination of the ^1H – ^{29}Si CP rate constants in the *p*-dichlorobenzene/ZSM-5 sorbate–zeolite complex which are used to determine the location and orientation of the guest molecule within the zeolite framework.

Experimental Section

Sample. A very highly siliceous and crystalline sample of ZSM-5 was used that had peak widths of about 0.1 ppm (8 to 10 Hz) in the ^{29}Si MAS NMR spectrum.¹² The zeolite–sorbate complex was prepared by accurately weighing out the appropriate amount of organic solid and mixing it with about 200 mg of calcined zeolite powder in a pre-scored glass ampule, giving a loading of approximately 3.5 molecules of pDCB per unit cell of ZSM-5. The ampule was evacuated on a vacuum line, flame-sealed, and then placed in an oven at about 80 to 100 °C for at least 12 h to equilibrate.

Solid-State NMR. Solid-state NMR experiments were carried out on a Bruker AVANCE DSX-400 NMR spectrometer operating at frequencies of 400.13 MHz for ^1H and 79.495 MHz for ^{29}Si , using a Bruker double-frequency CP MAS probe equipped with a standard 7 mm stator system from Doty Scientific. ^{29}Si chemical shifts were referenced to tetramethylsilane with use of Q_8M_8 ¹³ as a secondary reference and setting the highest field peak to -109.7 ppm. Low-temperature MAS was achieved by using pre-cooled nitrogen gas as the bearing gas and room-temperature air as the drive gas. The temperature was controlled and monitored by a heater–thermocouple system in the probe. The Hartmann–Hahn CP match condition for $^{29}\text{Si}\{^1\text{H}\}$ CP was initially set up on the Q_8M_8 reference sample and subsequently checked on the zeolite–sorbate sample itself. The power levels which gave the maximum of a relatively broad matching profile were approximately 30 kHz for both ^1H and ^{29}Si . ^1H decoupling applied during the acquisition time was found to have no noticeable effect on the width of the peaks in the ^{29}Si spectrum and was therefore not applied. All spectra were collected with use of a spinning rate of approximately 2 kHz. Additional experimental details for the individual spectra are provided in the figure captions.

Data Analysis. The deconvolution of the spectra and fitting of the CP and CP drain data were performed with programs written⁵ for Mathematica version 3.0.¹⁴

Results and Discussion

Cross-Polarization Dynamics. For a spin system consisting of relatively isolated *S* spins within an extended network of coupled *I* spins, the cross-polarization dynamics at the Hartmann–Hahn matching condition can be described in terms of spin thermodynamics in which “heat” flows between the *I* and *S* spin systems. Following the work of Mehring¹⁵ (which more recently has also been presented by others^{16–18}), the dynamics for cross polarization can be described by the set of coupled differential equations in eq 1 as indicated schematically in Figure 1

$$\begin{aligned} \frac{d\beta_S}{dt} &= -k_{IS}(\beta_S - \beta_I) - k_S\beta_S \\ \frac{d\beta_I}{dt} &= -\epsilon k_{IS}(\beta_I - \beta_S) - k_I\beta_I \end{aligned} \quad (1)$$

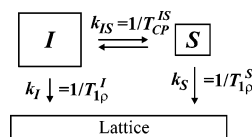


Figure 1. Schematic representation of the thermodynamic description of cross polarization.

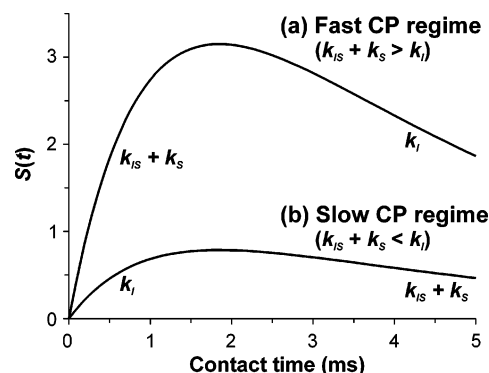


Figure 2. Dynamics of the observed *S* spin magnetization in a standard *I* → *S* cross polarization experiment: (a) fast CP regime in which the rate of *I* spin $T_{1\rho}$ relaxation is slow compared to the rate of cross polarization ($k_{IS} = 1000$ s^{−1}, $k_I = 250$ s^{−1}) and (b) slow CP regime in which the rate of *I* spin $T_{1\rho}$ relaxation is fast compared to the rate of cross polarization ($k_{IS} = 250$ s^{−1}, $k_I = 1000$ s^{−1}). The curves were generated by using eq 2, with $I_0 = 5$, $k_S = 0$, and the indicated values of k_{IS} and k_I .

where β_I and β_S are the inverse “spin temperatures” of the *I* and *S* spin systems, $\epsilon = (N_S S(S + 1))/(N_I I(I + 1))$ is the ratio of the “heat capacities” of the two spin reservoirs, $k_{IS} = 1/T_{CP}^{IS}$ is the rate constant for the “heat flow” between the *I* and *S* spins (the CP rate constant), and $k_I = T_{1\rho}^I$ and $k_S = T_{1\rho}^S$ are the rate constants for “heat flow” between the respective spins and the “lattice” (the inverse of the spin–lattice relaxation times in the rotating frame).

For the *I* → *S* cross-polarization experiment in which magnetization is transferred from the *I* spins to the observed *S* spins after an initial excitation pulse on the *I* spins, the initial conditions to the differential equations in eq 1 are $\beta_I(0) = \beta_I^0$ and $\beta_S(0) = 0$. If it is assumed that the *I* spins are abundant and the *S* spins are rare such that $\epsilon = 0$ and that the inverse spin temperature is proportional to the observed peak intensities, the expression for the observed *S* spin magnetization as a function of cross-polarization “contact time”, *t*, becomes

$$S(t) = I_0 \frac{k_{IS}}{(k_{IS} + k_S) - k_I} [\exp\{-k_I t\} - \exp\{-(k_{IS} + k_S)t\}] \quad (2)$$

where I_0 represents the initial *I* spin magnetization available for cross polarization and is equal to γ_I/γ_S times the magnetization obtained from a single pulse experiment on the *S* spins. The expression in eq 2 indicates that the observed *S* spin magnetization (the “CP curve”) grows to a maximum intensity and then decays, as shown in Figure 2.

It is often assumed that the $T_{1\rho}$ relaxation of the *S* spins is negligible, which is valid if k_S is much less than k_{IS} , but incorrect measurements of k_{IS} may result if this is not the case. In addition, when CP data are fit to extract the rate constants, it is usually assumed that the growth of the *S* spin magnetization depends on the CP rate constant (k_{IS}) and the decay depends on the *I* spin $T_{1\rho}$ relaxation rate constant (k_I). It is important to note that this assumption is only true in the fast CP regime ($k_{IS} + k_S >$

k_I) as shown in Figure 2a. In the slow CP regime, in which the rate of cross polarization is slow compared to the $T_{1\rho}$ relaxation of the I spins ($k_{IS} + k_S < k_I$), the rate constants for the growth and decay of the S spin magnetization are *reversed* from the usual assumptions:⁹ the rate of growth of the CP curve is governed by the rate constant k_I while the rate of decay is governed by the rate constant $k_{IS} + k_S$, as shown in Figure 2b. Essentially, the S spin magnetization grows until the I spin magnetization is depleted, after which the magnetization “flows” back from the S spins to the I spins where the magnetization is rapidly lost to the lattice by $T_{1\rho}$ relaxation of the I spins.

It is not possible to distinguish between the fast and slow CP regimes on the basis of a variable contact time CP curve alone. It is necessary to have additional information that could either come from knowledge of the nature of the sample under study or by comparison of the intensities to those of a quantitative single pulse spectrum. An important piece of information is often an independent measurement of the I spin $T_{1\rho}$ relaxation time. It has also been shown that the TORQUE experiment¹⁰ readily identifies the fast or slow CP regimes from the curvature of the TORQUE curves.^{9,11}

Under the slow CP regime, it is difficult, for a number of reasons, to obtain reliable values of the CP rate constant (k_{IS}) from $I \rightarrow S$ CP curves. The k_{IS} term is found in two parts of the expression for $S(t)$ in eq 2: in an exponential term and in the preexponential scaling factor. When the I spin $T_{1\rho}$ relaxation is fast, the exponential term in which k_{IS} is found describes the decay of the CP curve and this introduces problems for the measurement of the CP rate constants: First, the rate constant for the decay is $k_{IS} + k_S$ and nothing is known about k_S from a standard $I \rightarrow S$ CP experiment. Second, even if k_S can be assumed to be zero, it may be experimentally difficult to acquire enough reliable data points at long contact times to define this exponential decay and fit it since there is a limit in how long the contact pulses can be applied and the actual decay during this time period may well be small, increasing the error. In addition, the k_{IS} term is also present in the preexponential scaling factor. Since k_I is large with respect to $k_{IS} + k_S$ in the slow CP regime, this factor is approximately equal to $I_0(k_{IS}/k_I)$. Thus, a further difficulty in obtaining reliable k_{IS} values is that k_{IS} is very highly correlated to the I_0 value that also needs to be fit to the data. For data obtained under the slow CP regime where the decays in the CP curves are small, the fitting of k_{IS} values is mainly determined by the maximum intensities of the curves. Changing I_0 will give an entirely different set of k_{IS} values and nearly the same quality of fit. With respect to this last point, even though reliable *absolute* values of k_{IS} cannot be obtained from the CP curves in the slow CP regime, it is possible to obtain reliable *relative* values of k_{IS} since I_0 and k_I are expected to be constants that are identical (or almost so) for the CP curves of all the Si sites. However, it is possible to obtain reliable and absolute values of the CP rate constants in the slow CP regime by using a modification of the standard CP experiment as described below.

CP Drain Experiment. The cross-polarization drain experiment is a cross-depolarization experiment^{19–20} in which the excitation pulse and spin locking field are applied to the rare S spins and the “drain” or “depolarization” of magnetization from the S spins is observed with and without a Hartmann–Hahn matched field applied to the I spins, as illustrated in Figure 3. In this case, the initial conditions to the set of differential equations in eq 1 are $\beta_S(0) = \beta_S^0$ and $\beta_I(0) = 0$. Again, if it is assumed that the I spins are abundant and the S spins are rare, the expression for the observed S spin magnetization in a CP

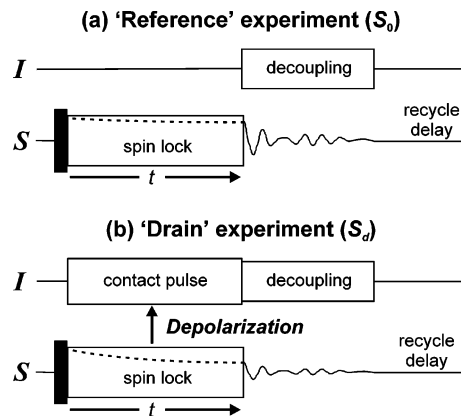


Figure 3. Pulse sequence diagrams for collecting the “reference” and “drain” spectra for the $S\{I\}$ cross-polarization drain experiments. In the “reference” experiments (S_0), the matched I spin radio frequency field is *not* applied during the spin lock of the S spins, while in the “drain” experiment (S_d) it is applied.

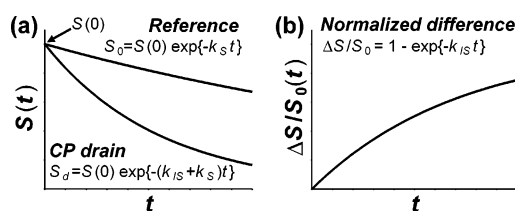


Figure 4. Cross-polarization dynamics in a $S\{I\}$ cross-polarization drain experiment: (a) reference (S_0) and drain (S_d) decays and (b) normalized difference curve ($\Delta S/S_0$).

drain experiment simplifies to:

$$S(t) = S(0) \exp\{-(k_S + k_{IS})t\} \quad (3)$$

The exponential decay resulting from the CP drain experiment *without* the contact pulse applied on the I spins (“reference” experiment S_0) is due entirely to S spin $T_{1\rho}$ relaxation and has the rate constant k_S since $k_{IS} = 0$ while the exponential decay resulting from the CP drain experiment *with* the contact pulse applied on the I spins (“drain” experiment S_d) has the rate constant $k_{IS} + k_S$ (see Figure 4a). The analysis of the CP drain dynamics can be simplified by plotting the data as a normalized difference plot²⁰ ($\Delta S/S_0$, where $\Delta S = S_0 - S_d$), such that the CP rate constant is the only variable to fit (see Figure 4b):

$$\Delta S/S_0(t) = 1 - \exp\{-k_{IS}t\} \quad (4)$$

In the slow CP regime, this analysis is clearly superior for measuring CP rate constants compared to fitting standard CP curves since these normalized difference curves depend *only* on k_{IS} . There is no dependence on the initial magnetization of the I spins (I_0), nor the $T_{1\rho}$ relaxation of the I and S spins (k_I and k_S). However, disadvantages of the CP drain experiment are that two separate experiments must be carried out and the data sets subtracted, resulting in a lowering of the S/N, and that the recycle delay of the experiment is determined by the T_1 relaxation time of the S nuclei, which is usually much longer than that of the I nuclei. However, the 90° pulse on the S spins could potentially be replaced by $I \rightarrow S$ cross polarization with the optimal contact time (when the I spin reservoir is depleted) so that the recycle time depends on the faster relaxation of the I nuclei.

CP Experiments on the Zeolite–Sorbate Complex. As mentioned in the Introduction, the $^1\text{H}–^{29}\text{Si}$ CP rate constants measured between ^1H nuclei of organic sorbate molecules and

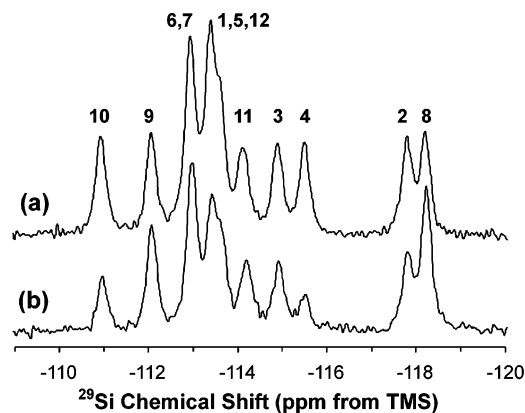


Figure 5. Comparison of (a) quantitative ^{29}Si MAS spectrum and (b) $^{29}\text{Si}\{^1\text{H}\}$ CP MAS spectrum of the low-loaded pDCB/ZSM-5 complex at 280 K. The quantitative spectrum was acquired with 32 scans and a 30 s recycle delay. The CP spectrum was acquired with 640 scans, a contact time of 15 ms, and a recycle delay of 2 s. ^1H decoupling was not applied during acquisition for either spectrum. The peaks were assigned from the correlations in a two-dimensional ^{29}Si INADEQUATE spectrum (not shown).

the ^{29}Si nuclei of the zeolite framework can be used to determine the location and orientation of these guest molecules in the cavities and channels of the host.^{1–5} Due to the presence of paramagnetic molecular oxygen in the cavities of the zeolite,⁸ the ^1H and ^{29}Si $T_{1\rho}$ relaxation times can be quite short while the CP time constants (T_{IS}) are quite long, due to the weak ^1H – ^{29}Si dipolar couplings and possible motions of the organic, such that $k_S \approx k_{IS} < k_I$. As a consequence of being in the slow CP regime, it is difficult to measure the ^1H – ^{29}Si CP rate constants by a standard ^1H – ^{29}Si CP experiment for the reasons described above and the CP drain experiment is therefore an important alternative for measuring the *absolute* CP rate constants in these zeolite–sorbate host–guest complexes. To illustrate this point, we present and discuss results obtained for the *p*-dichlorobenzene/ZSM-5 complex (pDCB/ZSM-5) with a loading of 3.5 molecules per unit cell at 280 K where the slow CP regime is shown to apply.

The ^{29}Si MAS and ^1H – ^{29}Si CP MAS NMR spectra of the pDCB/ZSM-5 complex are presented in Figure 5. The relative peak areas of the quantitative ^{29}Si MAS NMR spectrum (Figure 5a) reveal that there are 12 crystallographically unique Si sites in the structure. The peaks in the ^{29}Si spectrum were assigned to the Si sites in the structure by performing and analyzing a two-dimensional ^{29}Si INADEQUATE correlation experiment^{6,7} (spectrum not shown). The relative peak areas in the ^1H – ^{29}Si CP MAS spectrum (Figure 5b) indicate which ^{29}Si nuclei are close in space to the ^1H nuclei of the guest molecule, providing some qualitative information about the location of the pDCB molecule.

A series of variable contact time ^1H – ^{29}Si CP MAS experiments were carried out on the pDCB/ZSM-5 complex. The intensities for each Si peak were extracted, using peak positions and widths determined from the quantitative ^{29}Si spectrum, and plotted as functions of the contact time as shown in Figure 6. Since each ^{29}Si nucleus is being cross polarized from the same ^1H nuclei, these curves should have identical I_0 and k_I values and only differ in the value of k_{IS} (assuming $k_S = 0$). If one makes the “usual” assumption of “fast CP” in which the rate of growth in the CP curve is the CP rate constant (k_{IS}) while the decay is due to ^1H $T_{1\rho}$ relaxation (k_I), it is impossible to fit the curves with identical values of I_0 and k_I . It is only when it is realized that the CP dynamics are in the slow CP regime, where

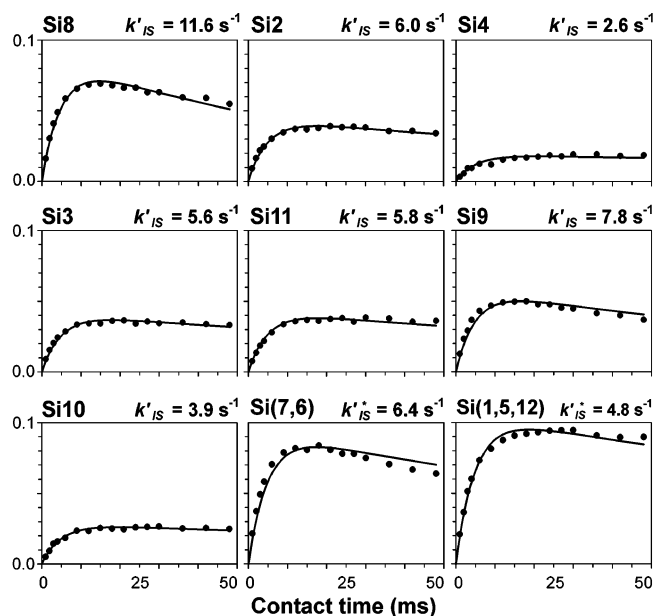


Figure 6. ^1H – ^{29}Si cross-polarization curves for the low-loaded pDCB/ZSM-5 complex at 280 K. The intensities (S_{CP}) are scaled with respect to a quantitative ^{29}Si MAS NMR spectrum. The curves were fit with eq 2 by using the relative CP rate constants indicated in each graph with $I_0 = 1.5$ and $k_I = 206 \text{ s}^{-1}$ (^1H $T_{1\rho} = 4.8 \text{ ms}$) and neglecting the ^{29}Si $T_{1\rho}$ relaxation ($k_S = 0 \text{ s}^{-1}$). The asterisk indicates an average value for the group of overlapping peaks. At each contact time, 640 scans were collected with a 2 s recycle delay.

the rate of growth is governed by the ^1H $T_{1\rho}$ relaxation with rate constant k_I and the rate of decay is governed by the CP rate constant (and ^{29}Si $T_{1\rho}$ relaxation rate constant k_S), that the data can be fit in a consistent manner with identical I_0 and k_I values for all the curves. The curves were all fit to eq 2 with the CP rate constants shown in Figure 6, using identical values of $I_0 = 1.5$ and $k_I = 206 \text{ s}^{-1}$ (corresponding to ^1H $T_{1\rho} = 4.8 \text{ ms}$) for each and assuming $k_S = 0$.

There are a number of important features of the CP dynamics in this slow CP regime. First, the cross-polarization process is very inefficient and this is a characteristic feature of the slow CP regime. The CP curves presented in Figure 6 are scaled with respect to the peak intensities obtained in the quantitative ^{29}Si MAS NMR spectrum, and only reach a maximum intensity of 0.02 to 0.07 of the quantitative ^{29}Si spectrum instead of being enhanced by a factor of up to $\gamma_{^1\text{H}}/\gamma_{^{29}\text{Si}} = 5$. This arises from the preexponential factor being approximately equal to $I_0(k_{IS}/k_I)$ when $k_{IS} \ll k_I$. Indeed, the measured values of k_{IS} are 1 or 2 orders of magnitude smaller than k_I . A second feature related to the preexponential factor is that the maximum intensity reached in the CP curve is strongly dependent on k_{IS} when $k_{IS} \ll k_I$ as is readily seen by comparing the CP curves in Figure 6. As a consequence, k_{IS} is very highly correlated to I_0 when fitting the CP curves and it is therefore difficult to obtain *absolute* values for k_{IS} from the CP curves in the slow CP regime. A third feature of the slow CP regime is that rates of growth of the CP curves and the contact times at which the maxima occur are the same in all the curves since they are governed by the fast ^1H $T_{1\rho}$ relaxation, while the rates of decay of the CP curves vary due to the different CP rate constants of the different Si sites. Another reason that it is difficult to obtain *absolute* values for k_{IS} is that the rate of decay of the CP curve is governed by $k_{IS} + k_S$ and not k_{IS} alone and that it is difficult to obtain enough data points to properly define this decay without using very long contact times. As a consequence of being unable to measure absolute rate constants, the CP rate

TABLE 1: Spectrum and Cross-Polarization Curve Fitting Parameters for the Low-Loaded pDCB/ZSM-5 Complex at 280 K

| Si | spectrum parameters ^a | | relaxation parameters ^b | | | CP time constants ^c | | CP rate constants ^d | |
|----|----------------------------------|------------|------------------------------------|------------|------------------|--------------------------------|----------------|--------------------------------|------------------------------|
| | shift (ppm) | width (Hz) | T_1 (s) | T_2 (ms) | $T_{1\rho}$ (ms) | T_{CP} (ms) | T'_{CP} (ms) | k_{IS} (s ⁻¹) | k'_{IS} (s ⁻¹) |
| 8 | -118.2 | 18.5 | 5.2 ± 0.2 | 20 ± 2 | 223 ± 9 | 72 ± 2 | 86 ± 1 | 13.9 ± 0.3 | 11.6 ± 0.1 |
| 2 | -117.8 | 19.8 | 2.1 ± 0.1 | 19 ± 1 | 113 ± 2 | 119 ± 2 | 167 ± 2 | 8.4 ± 0.1 | 6.0 ± 0.1 |
| 4 | -115.5 | 19.8 | 1.7 ± 0.1 | 20 ± 2 | 100 ± 2 | 303 ± 16 | 385 ± 10 | 3.3 ± 0.2 | 2.6 ± 0.1 |
| 3 | -114.9 | 20.3 | 1.8 ± 0.1 | 16 ± 1 | 108 ± 3 | 139 ± 4 | 179 ± 2 | 7.2 ± 0.2 | 5.6 ± 0.1 |
| 11 | -114.1 | 22.8 | 6.6 ± 0.4 | 24 ± 2 | 271 ± 20 | 152 ± 5 | 172 ± 3 | 6.6 ± 0.2 | 5.8 ± 0.1 |
| 9 | -112.1 | 18.1 | 1.8 ± 0.1 | 15 ± 1 | 94 ± 2 | 93 ± 3 | 128 ± 2 | 10.7 ± 0.3 | 7.8 ± 0.1 |
| 10 | -111.0 | 18.2 | 2.4 ± 0.1 | 26 ± 1 | 132 ± 2 | 179 ± 4 | 256 ± 4 | 5.6 ± 0.1 | 3.9 ± 0.1 |
| 12 | -113.6 | | | | | | | | |
| 1 | -113.4 | 17.6 | 2.6 ± 0.1 | 21 ± 1 | 130 ± 2 | 156 ± 2 | 208 ± 3 | 6.4 ± 0.1 | 4.8 ± 0.1 |
| 5 | -113.3 | | | | | | | | |
| 7 | -113.0 | | | | | | | | |
| 6 | -113.0 | 17.6 | 2.0 ± 0.1 | 17 ± 1 | 97 ± 1 | 109 ± 1 | 156 ± 2 | 9.2 ± 0.1 | 6.4 ± 0.1 |

^a Spectrum fitting parameters determined from a quantitative ²⁹Si MAS NMR spectrum. ^b Relaxation parameters determined from ²⁹Si saturation recovery (T_1), spin-echo (T_2), and spin locking ($T_{1\rho}$) experiments. ^c CP time constants determined from ²⁹Si{¹H} CP drain ($T_{CP} = 1/k_{IS}$) and standard CP ($T'_{CP} = 1/k'_{IS}$) experiments. ^d CP rate constants determined from ²⁹Si{¹H} CP drain (k_{IS}) and standard CP (k'_{IS}) experiments.

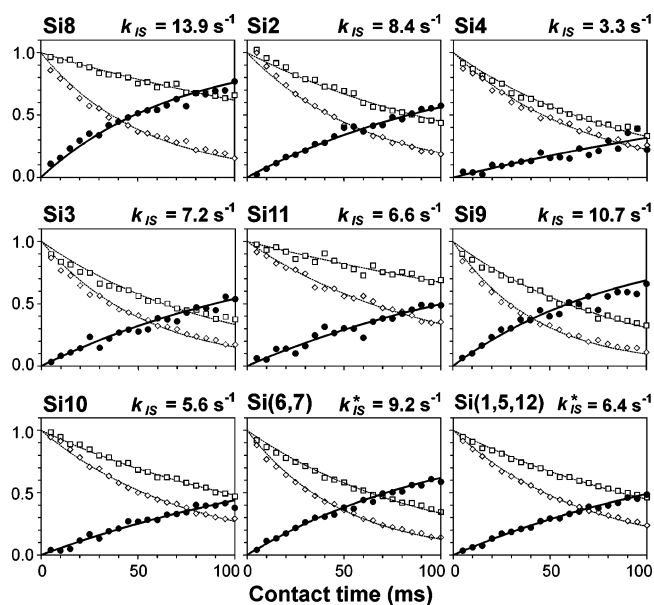


Figure 7. ²⁹Si{¹H} CP drain curves for the pDCB/ZSM-5 complex at 280 K. The “reference” ($S_0/S(0)$, open squares) and “drain” ($S_d/S(0)$, open diamonds) curves were fit to eqs 6 and 7, respectively. The normalized CP drain difference curves ($\Delta S/S_0$, filled circles) were fit to eq 8, using the CP rate constants indicated in each graph. The asterisk indicates an average value for the group of overlapping peaks. At each contact time, reference and drain spectra were acquired with 24 scans with a 25 s recycle delay.

constants obtained from the CP curves in the slow CP regime are considered to be *relative* values and are denoted by k'_{IS} .

To measure absolute CP rate constants, a series of variable contact time ²⁹Si{¹H} CP drain experiments were performed, with a “reference” and “drain” spectrum obtained at each contact time and the peak areas extracted with peak positions and widths determined from the quantitative ²⁹Si spectrum. Both the “reference” (S_0) and “drain” (S_d) curves for each ²⁹Si peak are presented in Figure 7 as open squares and diamonds, respectively. The “reference” curves show that the $T_{1\rho}$ relaxation rates vary for the different ²⁹Si nuclei and are similar in magnitude to the CP rate constants, suggesting that it may not be a valid assumption to neglect k_S when fitting the CP curves. This variation of the ²⁹Si $T_{1\rho}$ relaxation times probably arises from the varying proximities of the ²⁹Si nuclei to paramagnetic oxygen molecules which are localized in the zigzag channels.⁸ By plotting the data as normalized difference curves ($\Delta S/S_0$, filled circles), the curves depend *only* on k_{IS} (eq 4) and it is

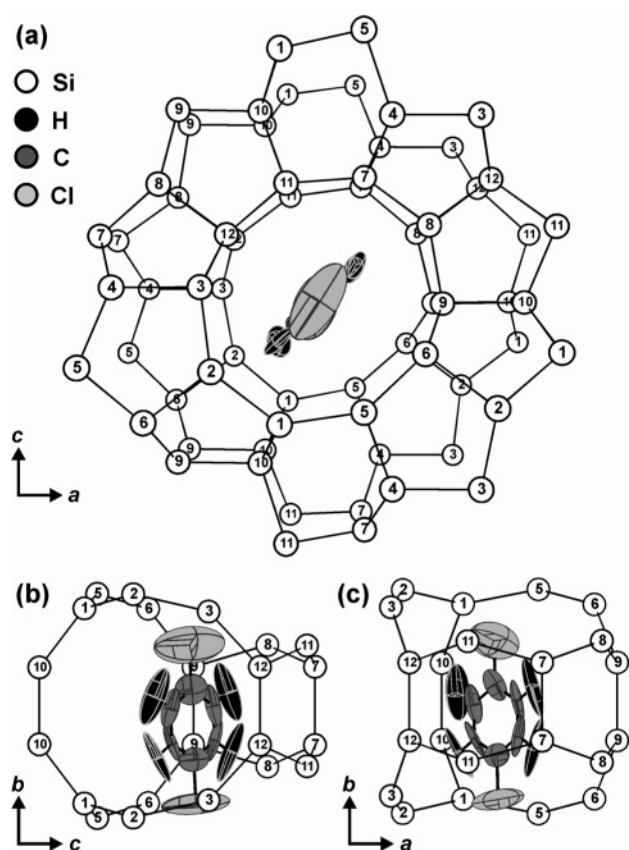


Figure 8. Average location (with error ellipsoids) of the pDCB molecule in ZSM-5 determined from the CP rate constants obtained from ²⁹Si{¹H} CP drain data collected at 280 K. Full details of this structure determination are found in ref 5. (a) View down the b -axis (straight channels), (b) view down the a -axis (zigzag channels), and (c) view down the c -axis.

therefore possible to obtain absolute CP rate constants. All of the peak-fitting and curve-fitting parameters, as well as relaxation times, are presented in Table 1.

The CP rate constants obtained from the CP curves (Figure 6) and from the CP drain curves (Figure 7) are compared in the last two columns of Table 1, which shows that the two sets of values are comparable. However, the rate constants obtained from the CP curves are consistently lower, probably due to the fact that they are highly correlated to I_0 . It is important to note that the relative ordering of the rate constants for the different Si sites is the same in both experiments. These measured CP

rate constants can be used to determine the location of the guest pDCB sorbate molecule in the zeolite framework by systematically searching the entire channel volume for locations and orientations of the pDCB molecule which give a high degree of linear correlation between the experimental k_{TS} values and the calculated ^1H – ^{29}Si second moments, as previously described. The exact details of the calculation for the pDCB/ZSM-5 complex are described elsewhere,⁵ but the final structure obtained from the NMR data is presented in Figure 8. This NMR-determined structure is in excellent agreement with the known structure from single-crystal X-ray diffraction.²¹ It should be noted that in this case, essentially the same structure is found when the relative CP rate constants obtained from the CP curves are used because the method used to solve the structure depends only on the relative values of the rate constants. However, proper identification of the correct CP rate constants will always be important, as will their absolute values.

Conclusions

In this paper, we have emphasized the importance of recognizing the “slow CP regime”, especially when the CP dynamics are being analyzed. This situation probably arises in many other systems besides zeolite host–guest complexes, especially those in which the heteronuclear dipolar interactions are predictably weak such as host–guest complexes in general and adsorbant–surface complexes and interfacial interactions in general. We have also shown the measurement of CP rate constants in the slow CP regime is not straightforward from standard CP curves and is best accomplished by using CP drain experiments where this is possible. Last, we have demonstrated the importance of these observations by describing the structure determination of a zeolite–sorbate complex from the (correctly) measured ^1H – ^{29}Si CP rate constants, the details of which are presented elsewhere.⁵

Acknowledgment. The authors thank the Natural Sciences and Engineering Council of Canada for Operating and Equipment grants (C.A.F.) and for the award of a Postgraduate Fellowship (D.H.B.).

References and Notes

- (1) Fyfe, C. A.; Diaz, A. C.; Lewis, A. R.; Chézeau, J.-M.; Grondey, H.; Kokotailo, G. T. In *Solid State NMR Spectroscopy of Inorganic Materials*; Fitzgerald, J. J., Ed.; ACS Symp. Ser., No. 717; American Chemical Society: Washington, DC, 1999; pp 283–304.
- (2) Fyfe, C. A.; Diaz, A.; Grondey, H.; Lewis, A. R.; Förster, H. *J. Am. Chem. Soc.* **2005**, *127*, 7543.
- (3) Diaz, A. Investigation of the three-dimensional structures of zeolite molecular sieves by high-resolution solid-state NMR, Ph.D. Thesis, Department of Chemistry, University of British Columbia, Vancouver, Canada, 1998.
- (4) Lewis, A. Location of guest species in zeolites by solid-state NMR, Ph.D. Thesis, Department of Chemistry, University of British Columbia, Vancouver, Canada, 1998.
- (5) Brouwer, D. H. Location, dynamics, and disorder of guest species in zeolite frameworks studied by solid-state NMR and X-ray diffraction, Ph.D. Thesis, Department of Chemistry, University of British Columbia, Vancouver, Canada, 2003.
- (6) Fyfe, C. A.; Grondey, H.; Feng, Y.; Kokotailo, G. T. *J. Am. Chem. Soc.* **1990**, *112*, 8812.
- (7) Brouwer, D. H. *J. Magn. Reson.* **2003**, *164*, 10.
- (8) Fyfe, C. A.; Brouwer, D. H. *J. Am. Chem. Soc.* **2004**, *126*, 1306.
- (9) Klur, I.; Jacquinet, J.-F.; Brunet, F.; Charpentier, T.; Virlet, J.; Schneider, C.; Tekely, P. *J. Phys. Chem. B* **2000**, *104*, 10162.
- (10) Tekely, P.; Gerardy, V.; Palmas, P.; Canet, D.; Retournard, A. *Solid State Nucl. Magn. Reson.* **1995**, *4*, 361.
- (11) Gardiennet, C.; Tekely, P. *J. Phys. Chem. B* **2002**, *106*, 8928.
- (12) Fyfe, C. A.; O'Brien, J. H.; Strobl, H. *Nature* **1987**, *326*, 281.
- (13) Hoebbel, D.; Wieker, W. *Z. Anorg. Allg. Chem.* **1971**, *384*, 43.
- (14) Agaskar, P. A. *Inorg. Chem.* **1990**, *29*, 1603.
- (15) Wolfram, S. *Mathematica: A System for Doing Mathematics by Computer*, v. 3.0; Wolfram Media: Champaign, IL, 1996.
- (16) Mehring, M. *Principles of High-Resolution NMR in Solids*, 2nd ed.; Springer-Verlag: Berlin, Germany, 1983.
- (17) Klein Douwel, C. H.; Maas, W. E. J. R.; Veeman, W. S.; Werumeus Buning, G. H.; Vankan, J. M. *J. Macromolecules* **1990**, *23*, 406.
- (18) Ando, S.; Harris, R. K.; Reinsberg, S. A. *J. Magn. Reson.* **1999**, *141*, 91.
- (19) Kolodziejski, W.; Klinowski, J. *Chem. Rev.* **2002**, *102*, 613.
- (20) Schaefer, J.; McKay, R. A.; Stejskal, E. O. *J. Magn. Reson.* **1979**, *34*, 443.
- (21) Stejskal, E. O.; Schaefer, J.; McKay, R. A. *J. Magn. Reson.* **1984**, *57*, 471.
- (22) van Koningsveld, H.; Jansen, J. C.; de Man, A. J. M. *Acta Crystallogr.* **1996**, *B52*, 131.